J. Fluid Mech. (2024), *vol*. 996, A17, doi:10.1017/jfm.2024.625

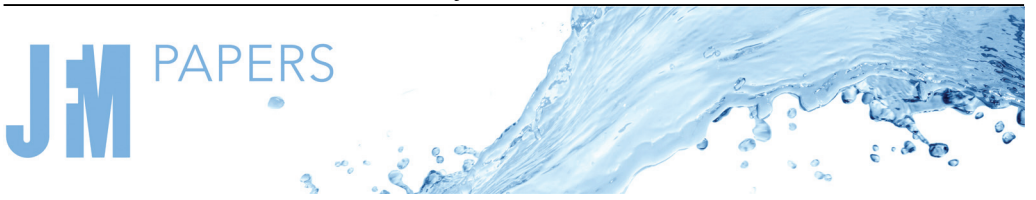

Inviscid jets driven by pressure maxima

J.R. Ockendon[1],† **and H. Ockendon**[1]

[1]Mathematical Institute, University of Oxford, Woodstock Road, Oxford OX2 6GG, UK

(Received 20 April 2024; revised 7 June 2024; accepted 12 June 2024)

Recent numerical calculations have revealed the existence of fast jets in inviscid fluids when a pressure maximum exists close to a free boundary. This paper describes two-dimensional and axisymmetric configurations for which asymptotic analysis suggests that such jets can become infinitely long in finite time.

Key words: jets

1. Introduction

Although the theory of inviscid liquid jets has a long history, much of the literature has concerned steady flows, often driven by gravity. However, there are many papers concerning unsteady jets, see for example Longuet-Higgins (1972) and Longuet-Higgins (1975) and, more recently, jets caused by the impact of a solid on an initially planar interface (King & Needham 1994; Needham, Billingham & King 2007; Iafrati & Korobkin 2008). When the solid is flat, very high-speed jets can be created at the corner of the impactor but only very recently has it been shown that such jets can occur spontaneously at a free surface and this is the phenomenon that has driven the research described in this paper.

The computations of Scolan (2023) and Scolan & Etienne (2021) have revealed the onset of localised high-speed so-called 'critical' jets on the underside of breaking gravity waves, the time scale of the jet evolution being much shorter than that of the gravity wave. Their computations revealed the local evolution of the fluid velocity and pressure in some detail and, in particular, the existence of a pressure maximum in close proximity to the free surface, which produces local pressure gradients which are two orders of magnitude greater than the average value. The dramatic effects of such pressure maxima are apparent in shaped charges and in the free boundary configuration considered in Cooker (2002).

Our aim in this paper is to describe a simple model for critical jet initiation in two-dimensional and axisymmetric flow, neglecting gravity effects. We suppose that, for

† Email address for correspondence: ock@maths.ox.ac.uk

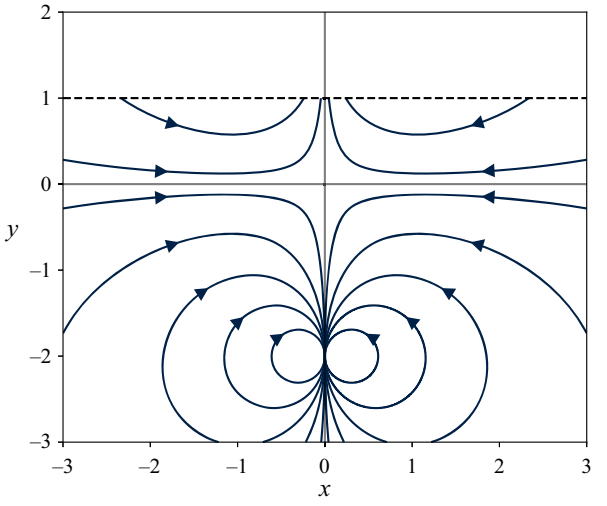

Figure 1. The initial streamlines for $y \leq 1$ when $d = 2$.

time $t < 0$, the liquid flow is that of a stagnation point at the origin created by remote dipoles at equal distances d above and below the stagnation point, as illustrated in figure 1. Such configurations are common in, say, the study of water entry problems, because the resulting velocity field tends to zero at infinity.

With $d > 1$, we now generate a free-boundary problem by instantaneously removing all the liquid above the line $y = 1$ at time $t = 0$ and assume that for $t > 0$ the remaining liquid is exposed to a vacuum. Even for this configuration, there do not seem to be any exact solutions for finite values of d. However, when d is large, and also when $d - 1$ is small, the evolution of the jet can be revealed by asymptotic analysis, at least for certain times. The configuration is probably physically unrealistic but it models the pressure maximum and is susceptible to asymptotic analysis, as will be seen in §§ 2 and 3. Moreover, the pressure is not initially zero on $y = 1$ as it is in Scolan (2023) and Scolan & Etienne (2021). Nonetheless, it is hoped that our explicit asymptotic solutions will provide useful validation of numerical predictions of rapid jet formation.

In § 2, we will first consider the two-dimensional problem when $d \to \infty$ and we show that the boundary moves to infinity in finite time, henceforth referred to as blow-up. When the dipole is present, small-time solutions are presented that show how a jet begins to evolve, and asymptotic results are then obtained, first for large values of d and, briefly, for small values of $(d - 1)$. Then we repeat this analysis for the axisymmetric version of the problem.

2. The two-dimensional problem

The sudden jump in pressure at $t = 0$ will cause a jump in acceleration in the liquid, which will then flow according to the following normalised model for the potential $\phi(x, y, t)$ and the free surface $y = f(x, t)$, assumed single valued. Also, ϕ and its first spatial derivatives will be continuous at $t = 0$. Then, for $t > 0$,

$$\frac{\partial^2 \phi}{\partial x^2} + \frac{\partial^2 \phi}{\partial y^2} = 0, \quad y \leq f(x, t), \tag{2.1}$$

where, on $y = f(x, t)$, the dynamic boundary condition for the pressure p is

$$-p = \frac{\partial \phi}{\partial t} + \frac{1}{2}|\nabla \phi|^2 = 0, \tag{2.2}$$

and we have taken the pressure to be zero at infinity when d is finite. The kinematic boundary condition on $y = f(x, t)$ is

$$\frac{\partial f}{\partial t} + \frac{\partial \phi}{\partial x}\frac{\partial f}{\partial x} = \frac{\partial \phi}{\partial y}. \tag{2.3}$$

Also ϕ has a suitably normalised dipole singularity at $(0, -d)$ and the initial conditions are

$$\phi(x, y, 0) = \frac{d^3}{2}\left(\frac{y+d}{x^2+(y+d)^2} - \frac{y-d}{x^2+(y-d)^2} - \frac{2}{d}\right) \tag{2.4}$$

for $y \leq 1$ and

$$f(x, 0) = 1. \tag{2.5}$$

2.1. *Solutions for large d*

When we formally set $d = \infty$, then (2.4) becomes $\phi(x, y, 0) = y^2 - x^2$ and we can write

$$\phi = A(t)(y^2 - x^2) + B(t), \quad f = F(t), \tag{2.6}$$

where $A(0) = 1, B(0) = 0$ and $F(0) = 1$. Thus, from (2.2) and (2.3),

$$\frac{\mathrm{d}A}{\mathrm{d}t} = 2A^2, \quad \frac{\mathrm{d}F}{\mathrm{d}t} = 2AF \quad \text{and} \quad \frac{\mathrm{d}B}{\mathrm{d}t} = -4A^2F^2, \tag{2.7a–c}$$

and we find that $A = F = 1/(1-2t), B = -2/(3(1-2t)^3) + \frac{2}{3}$, which is one case of the family of explicit solutions described by Longuet-Higgins (1972). The pressure p is given by

$$p = \frac{4(F^2 - y^2)}{(1-2t)^2}, \tag{2.8}$$

having jumped from $-2(x^2+y^2)$ to $4(1-y^2)$ at $t = 0$. Thus, not only does blow-up occur when $t = \frac{1}{2}$ but the pressure has a maximum that increases with time on the whole x-axis. We also note that when the stagnation-point flow is reversed so that $A(0) = -1$, the pressure still has a maximum on $y = 0$ but $F(t) = -A(t) = 1/(1+2t)$ and thus the free boundary moves towards $y = 0$ as $t \to \infty$.

2.1.1. *The case of d large and* $0 < t < \frac{1}{2}$

A limit that leads to tractable asymptotic solutions occurs when d is large. In this case we write $\epsilon = 1/d$ and, when x, y are $O(1)$, the solution (2.6) will hold to lowest order. This is no longer true as $|x| \to \infty$ and so we need to introduce an outer region which is of width $O(\epsilon^{-1})$ in the x-direction while y remains of $O(1)$. Thus with $X = \epsilon x$, $\Phi = \epsilon^2 \phi$, the

problem becomes

$$\epsilon^2 \frac{\partial^2 \Phi}{\partial X^2} + \frac{\partial^2 \Phi}{\partial y^2} = 0 \tag{2.9}$$

with, on the free boundary, now denoted by $y = F(X, t)$,

$$\epsilon^2 \left(\frac{\partial \Phi}{\partial t} + \frac{1}{2} \left(\frac{\partial \Phi}{\partial X} \right)^2 \right) + \frac{1}{2} \left(\frac{\partial \Phi}{\partial y} \right)^2 = 0, \tag{2.10}$$

and

$$\epsilon^2 \left(\frac{\partial F}{\partial t} + \frac{\partial \Phi}{\partial X} \frac{\partial F}{\partial X} \right) = \frac{\partial \Phi}{\partial y}. \tag{2.11}$$

Also, at $t = 0$, expanding the term in brackets in (2.4) for large d and using (2.5) gives

$$F = 1 \quad \text{and} \quad \Phi \sim -\frac{X^2}{1 + X^2} + O(\epsilon^2). \tag{2.12a,b}$$

Finally, matching with the solution (2.6) gives that, as $X \to 0$,

$$\Phi \sim -\frac{X^2}{1 - 2t}, \quad F \sim \frac{1}{1 - 2t}. \tag{2.13a,b}$$

When we now expand in the form

$$\Phi \sim \Phi_0 + \epsilon^2 \Phi_1 + \cdots, \quad F \sim F_0 + \epsilon^2 F_1 + \cdots, \tag{2.14a,b}$$

we find that, for some functions α and β,

$$\Phi_0 = \alpha(X, t) y + \beta(X, t), \tag{2.15}$$

where, from (2.12*b*), $\alpha(X, 0) = 0$ and $\beta(X, 0) = -(X^2/(1 + X^2))$. Then conditions (2.10) and (2.11) imply that $\alpha(X, t) = 0$ and so Φ_0 is independent of y. In order to determine Φ_0, we need to proceed to the second-order terms in (2.10) which reveals that

$$\frac{\partial \Phi_0}{\partial t} + \frac{1}{2} \left(\frac{\partial \Phi_0}{\partial X} \right)^2 = 0, \tag{2.16}$$

with the initial condition from (2.12*b*) that

$$\Phi_0 = -\frac{X^2}{1 + X^2} \quad \text{at } t = 0. \tag{2.17}$$

Charpit's equations for (2.16) show that $P = \partial \Phi_0 / \partial t$ and $Q = \partial \Phi_0 / \partial X$ are constant on the characteristics of (2.16) through the point $X = X_0$, $t = 0$ and these characteristics are

the particle paths given by $\mathrm{d}X/\mathrm{d}t = Q$. Hence

$$Q = \frac{-2X_0}{(1+{X_0}^2)^2}, \tag{2.18}$$

and

$$\Phi_0 = \frac{2{X_0}^2 t}{(1+{X_0}^2)^4} - \frac{{X_0}^2}{1+{X_0}^2}, \tag{2.19}$$

where

$$X = Qt + X_0 = X_0 - \frac{2X_0 t}{(1+{X_0}^2)^2}. \tag{2.20}$$

The free surface can now be derived from (2.11) in the form

$$\frac{\partial F_0}{\partial t} + \frac{\partial \Phi_0}{\partial X}\frac{\partial F_0}{\partial X} = \frac{\partial \Phi_1}{\partial y} \quad \text{on } y = F_0, \tag{2.21}$$

where

$$\Phi_1 = -\frac{1}{2}y^2\frac{\partial^2 \Phi_0}{\partial X^2} + c_0(X,t)y + c_1(X,t), \tag{2.22}$$

and c_0 and c_1 are functions of integration. However, the fact that the velocity is zero at infinity ensures that $c_0(X,t) = 0$.

We note that the characteristics of (2.21) are also the particle paths. Hence it is now convenient to change from Eulerian coordinates (X,t) to Lagrangian coordinates (X_0,t). Using (2.20), we see that, in Lagrangian coordinates with t held constant,

$$\frac{\partial X}{\partial X_0} = 1 - \frac{2t(1-3{X_0}^2)}{(1+{X_0}^2)^3}. \tag{2.23}$$

Hence, from (2.18),

$$\frac{\partial^2 \Phi_0}{\partial X^2} = \frac{\partial Q}{\partial X_0}\Big/\frac{\partial X}{\partial X_0} = \frac{2(3{X_0}^2-1)}{(1+{X_0}^2)^3 - 2t(1-3{X_0}^2)}, \tag{2.24}$$

and (2.21) becomes

$$\left(1 - \frac{2t(1-3{X_0}^2)}{(1+{X_0}^2)^3}\right)\frac{\partial F_0}{\partial t} = \frac{2(1-3{X_0}^2)}{(1+{X_0}^2)^3}F_0. \tag{2.25}$$

Then, using the condition $F_0 = 1$ at $t = 0$, we obtain

$$F_0 = \frac{1}{\left(1 - \dfrac{2t(1-3{X_0}^2)}{(1+{X_0}^2)^3}\right)}, \tag{2.26}$$

where (2.20) relates X, t and X_0. Note that (2.26) and (2.19) match with (2.13*a*,*b*) as $X \to 0$ with $t < 1/2$. Typical profiles for F_0 are shown in figure 2.

It is relatively easy to show that F_0 always has a minimum at $X_0 = 1$ and then approaches 1 from below as $|X_0| \to \infty$, as shown in figure 2. Most importantly, when $X_0 = 0$ we have $X = 0$ and $F_0 = 1/(1-2t)$ and so the extreme tip of the jet goes to infinity in finite time

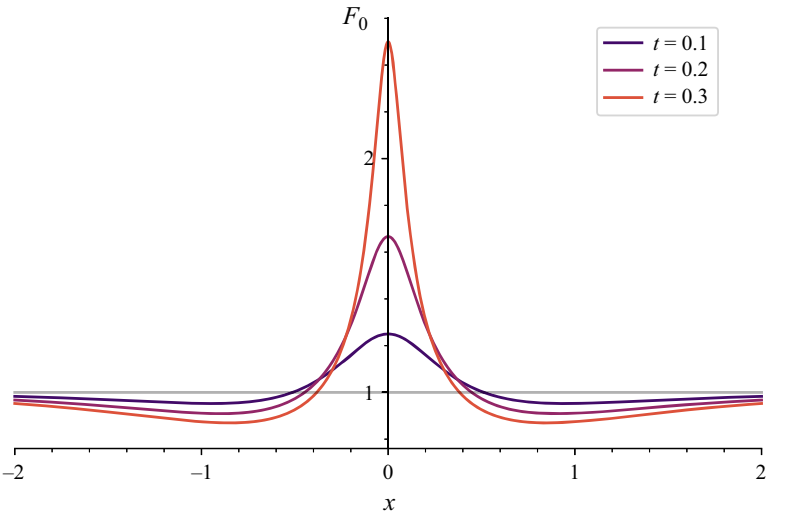

Figure 2. Value of F_0 defined by (2.26), plotted as a function of X for $t = 0, 0.1, 0.2, 0.3$.

in the large d limit. Moreover, using (2.2), (2.16) and (2.22), we find that, to lowest order in ϵ,

$$-p = -\frac{1}{2}y^2\frac{\partial^3\Phi_0}{\partial X^2\partial t} + \frac{\partial c_1}{\partial t} + \frac{\partial\Phi_0}{\partial X}\left(-\frac{1}{2}y^2\frac{\partial^3\Phi_0}{\partial X^3} + \frac{\partial c_1}{\partial X}\right) + \frac{1}{2}y^2\left(\frac{\partial^2\Phi_0}{\partial X^2}\right)^2. \tag{2.27}$$

Using (2.16), this reduces to

$$-p = y^2\left(\frac{\partial^2\Phi_0}{\partial X^2}\right)^2 + \frac{\partial c_1}{\partial t} + \frac{\partial\Phi_0}{\partial X}\frac{\partial c_1}{\partial X}. \tag{2.28}$$

Since $p = 0$ on $y = F_0$, this means that

$$\frac{\partial c_1}{\partial t} + \frac{\partial\Phi_0}{\partial X}\frac{\partial c_1}{\partial X} = -{F_0}^2\left(\frac{\partial^2\Phi_0}{\partial X^2}\right)^2, \tag{2.29}$$

and hence that

$$p = \left(\frac{\partial^2\Phi_0}{\partial X^2}\right)^2({F_0}^2 - y^2). \tag{2.30}$$

Thus, pressure maxima in this regime can only occur on $y = 0$.

Using (2.24), we see that the pressure on $y = 0$ is a function of X, as shown in figure 3. Moreover, since X is a monotone increasing function of X_0, p will now have two maxima in $X \geq 0$, with the maximum at $X = 0$ being increasingly dominant as $t \to \frac{1}{2}$. We remark that the weaker maximum is generated by our initial conditions and is not associated with a stagnation-point flow.

The behaviour revealed in figure 3 enables us to draw the isobars in $X \geq 0$, $y \geq 0$ as shown in figure 4. The isobars in $y < 0$ are the mirror image of those in $y > 0$ until the zero-pressure isobar is reached and the pressure is everywhere negative below this isobar.

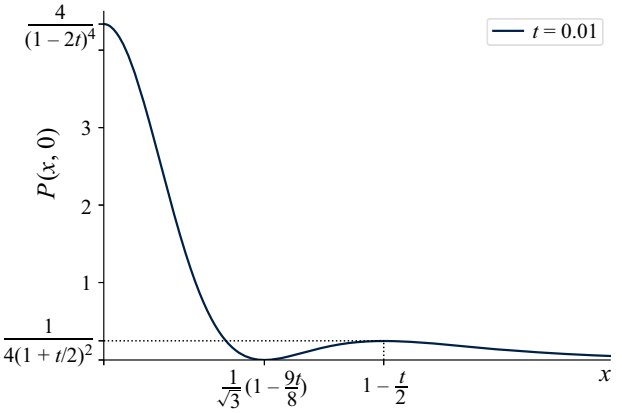

Figure 3. Value of $p(X, 0)$ plotted from (2.30) for $t = 0.01$.

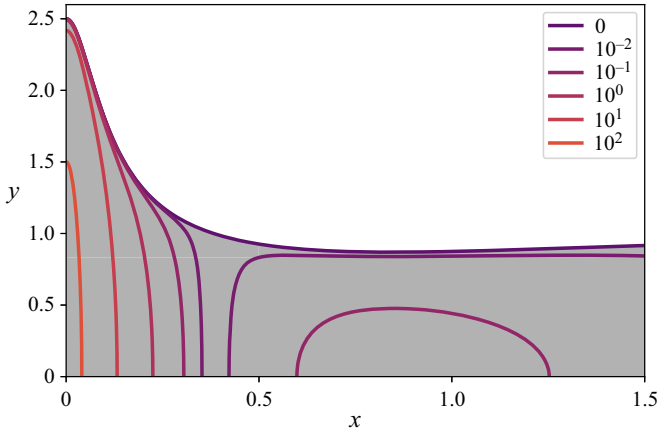

Figure 4. Isobars of $p(X, y)$ for $t = 0.3$ when $y > 0$; the fluid region is shaded.

2.1.2. *The limit as* $t \uparrow \frac{1}{2}$

We observe that, when X_0 and $\frac{1}{2} - t = \tau$ are small, (2.19) and (2.26) give

$$X \sim 2X_0(\tau + {X_0}^2), \quad F_0 \sim \frac{1}{2\tau + 6{X_0}^2}, \quad \Phi_0 \sim -{X_0}^2(2\tau + 3{X_0}^2). \tag{2.31a–c}$$

Hence, the solution is singular as $X_0, \tau \to 0$ and rapid changes are expected when τ and ${X_0}^2$ are small and comparable. If we assume that $\tau = O(\hat{\epsilon}^2)$ and $X_0 = O(\hat{\epsilon})$ for some small parameter $\hat{\epsilon}$, then the appropriate scalings in this region are

$$x = O\left(\frac{\hat{\epsilon}^3}{\epsilon}\right), \quad y = O(\hat{\epsilon}^{-2}), \quad \phi = O\left(\frac{\hat{\epsilon}^4}{\epsilon^2}\right), \tag{2.32a–c}$$

and this leads to a region where Laplace's equation (2.1) holds if $\hat{\epsilon} = \epsilon^{1/5}$. Thus we write

$$\tau = \epsilon^{2/5}\hat{\tau}, \quad x = \epsilon^{-2/5}\hat{x}, \quad y = \epsilon^{-2/5}\hat{y}, \quad f = \epsilon^{-2/5}\hat{f} \quad \text{and} \quad \phi = \epsilon^{-6/5}\hat{\phi}. \tag{2.33a–e}$$

The resulting free-boundary problem is equivalent to the full problem (2.1) with boundary conditions (2.2) and (2.3) but with the solution matching with (2.31*a–c*) as $\hat{x} \to \infty$. If we

let $X_0 \to 0$ in (2.31*a–c*) while keeping τ constant we see that, for $t < \frac{1}{2}$,

$$\hat{\phi} \sim -\frac{\hat{x}^2}{2\hat{\tau}} \quad \text{and} \quad \hat{f} \sim \frac{1}{2\hat{\tau}}, \tag{2.34a,b}$$

as $\hat{x} \to \infty$. As $\hat{\tau} \to \infty$, we need to match with (2.6) and hence the solution is

$$\hat{\phi} = \frac{\hat{y}^2 - \hat{x}^2}{2\hat{\tau}} - \frac{1}{12\hat{\tau}^3}, \quad \hat{f} = \frac{1}{2\hat{\tau}}, \tag{2.35a,b}$$

which is equivalent to the limit of (2.6) as $t \uparrow 1/2$. Thus, to lowest order in ϵ, the jet extends to infinity at $\hat{\tau} = 0$. As noted after (2.8), the lowest-order pressure maintains a maximum along $y = 0$.

2.2. *The case of d finite and $t \ll 1$*

(i) $d > 1$ We will consider only the small-time solution of (2.1), (2.2), (2.3) and (2.4) for $d > 1$. Assuming a smooth dependence on time, we seek expansions of the form

$$\phi \sim \phi(x, y, 0) + t\phi_1(x, y) + \cdots, \tag{2.36}$$

and

$$f \sim 1 + tf_1(x) + \cdots. \tag{2.37}$$

Then we find that

$$f_1 = \frac{\partial \phi(x, y, 0)}{\partial y}|_{y=1} = \frac{-2d^4(3x^4 + 2(1 + d^2)x^2 - (1 - d^2)^2)}{(x^2 + (1 - d)^2)^2(x^2 + (1 + d)^2)^2}, \tag{2.38}$$

and we see that the free surface immediately adopts the jet profile shown in figure 5. The zeros of f_1 are where $3x^2 = 2\sqrt{1 - d^2 + d^4} - 1 - d^2$ and $f_1(0) = 2d^4/(1 - d^2)^2$. However, the lowest-order pressure can only be calculated by finding ϕ_1, which involves solving a complicated potential problem which will not be addressed here. We also note that figure 5 has the same geometrical features as were seen in the longer-time solutions shown in figure 2.

(ii) $d \downarrow 1$ The profile (2.38) tends to infinity as $x \to 0$ when $d = 1$ and hence, to understand what happens as $\delta = d - 1$ tends to zero, we expand (2.4) by writing

$$y = 1 + \delta\tilde{y}, \quad x = \delta\tilde{x}, \tag{2.39a,b}$$

and, noting that there is only one effective dipole in this region, (2.38) gives that, at $t = 0$,

$$\phi \sim -\frac{\tilde{y} - 1}{2\delta(\tilde{x}^2 + (\tilde{y} - 1)^2)} + O(1). \tag{2.40}$$

Hence, for t of $o(\delta^2)$,

$$f_1 \sim -\frac{(\tilde{x}^2 - 1)}{2\delta^2(1 + \tilde{x}^2)^2} + O(1). \tag{2.41}$$

In this short time-scale regime, the free boundary is still of the same form as in figure 5 and the length of the jet is $t/2\delta^2$ while its width is of $O(\delta)$.

In summary, we have shown that, when d is either near to unity or tends to infinity, the formal asymptotic analysis suggests that the interface tends to infinity in a finite

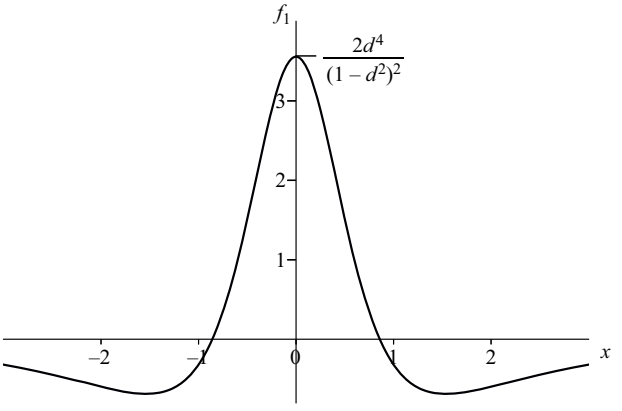

Figure 5. Value of f_1 plotted as a function of x from (2.38).

time. In both cases the free surface is focussed into a jet which contains 4 inflection points, as shown in figures 2 and 5.

We now turn to the axisymmetric case, which will be found to lead to similar consequences but with even stronger jet accelerations.

3. The axisymmetric problem

This section will describe the straightforward generalisation of the asymptotic analysis in § 2 to the case of axisymmetric jets with a far-field dipole. Only the principal equations and results will be stated by using relevant analogies from § 2; the same notation will be used for the velocity potential and the free surface profile.

In radial polar coordinates (r, z), the model is

$$\frac{\partial^2\phi}{\partial r^2} + \frac{1}{r}\frac{\partial\phi}{\partial r} + \frac{\partial^2\phi}{\partial z^2} = 0, \quad z < f(r,t), \tag{3.1}$$

with, on $z = f(r, t)$,

$$\frac{\partial\phi}{\partial t} + \frac{1}{2}\left(\left(\frac{\partial\phi}{\partial r}\right)^2 + \left(\frac{\partial\phi}{\partial z}\right)^2\right) = 0, \tag{3.2}$$

and

$$\frac{\partial f}{\partial t} + \frac{\partial\phi}{\partial r}\frac{\partial f}{\partial r} = \frac{\partial\phi}{\partial z}. \tag{3.3}$$

Also, at $t = 0$,

$$\phi = \frac{1+\epsilon z}{6\epsilon^2((1+\epsilon z)^2+\epsilon^2 r^2))^{3/2}} + \frac{1-\epsilon z}{6\epsilon^2((1-\epsilon z)^2+\epsilon^2 r^2))^{3/2}} - \frac{1}{3\epsilon^2}, \tag{3.4}$$

which is the analogue of (2.4) with $\epsilon = d^{-1}$, and

$$f = 1. \tag{3.5}$$

When $\epsilon = 0$, the analogue of (2.6) is

$$\phi = \frac{z^2 - r^2/2}{1-t} - \frac{3}{5(1-t)^5} + \frac{3}{5}, \quad f = \frac{1}{(1-t)^2}. \tag{3.6}$$

Thus the eventual acceleration of the interface is an order of magnitude greater than in the two-dimensional case.

3.1. *The solution for small* ϵ

When $z = O(1)$ and $r = O(\epsilon^{-1})$, we write $r = R/\epsilon$ and $\phi = \Phi/\epsilon^2$ so that

$$\frac{\partial^2 \Phi}{\partial z^2} + \epsilon^2 \left(\frac{\partial^2 \Phi}{\partial R^2} + \frac{1}{R} \frac{\partial \Phi}{\partial R} \right) = 0, \tag{3.7}$$

with, on $z = F(R, t)$,

$$\frac{1}{2} \left(\frac{\partial \Phi}{\partial z} \right)^2 + \epsilon^2 \left(\frac{1}{2} \left(\frac{\partial \Phi}{\partial R} \right)^2 + \frac{\partial \Phi}{\partial t} \right) = 0, \tag{3.8}$$

and

$$\frac{\partial \Phi}{\partial z} = \epsilon^2 \left(\frac{\partial F}{\partial t} + \frac{\partial \Phi}{\partial R} \frac{\partial f}{\partial R} \right). \tag{3.9}$$

Writing

$$\Phi \sim \Phi_0 + \epsilon^2 \Phi_1 + \cdots, \tag{3.10}$$

and

$$F \sim F_0 + \epsilon^2 F_1 + \cdots, \tag{3.11}$$

the lowest-order solution gives Φ_0 as a function of R, t only, and such that

$$\frac{\partial \Phi_0}{\partial t} + \frac{1}{2} \left(\frac{\partial \Phi_0}{\partial R} \right)^2 = 0. \tag{3.12}$$

The initial conditions are

$$\Phi_0(R, 0) = \frac{1}{3(1 + R^2)^{3/2}} - \frac{1}{3}, \quad F_0(0) = 1, \tag{3.13}$$

and the analogue of (2.21) is

$$\frac{\partial F_0}{\partial t} + \frac{\partial \Phi_0}{\partial R} \frac{\partial F_0}{\partial R} = \frac{\partial \Phi_1}{\partial z} = -\left(\frac{\partial^2 \Phi_0}{\partial R^2} + \frac{1}{R} \frac{\partial \Phi_0}{\partial R} \right) F_0 - c_0(R, t), \tag{3.14}$$

and again $c_0(R, t)$ has to vanish since there is no mean flow at infinity. The relevant solution of (3.12) is

$$\Phi_0 = \frac{{R_0}^2 t}{2(1 + {R_0}^2)^5} + \frac{1}{3(1 + {R_0}^2)^{3/2}} - \frac{1}{3}, \tag{3.15}$$

where

$$R = R_0 - \frac{R_0 t}{(1 + {R_0}^2)^{5/2}}, \tag{3.16}$$

and R_0 is a parameter analogous to X_0 in two dimensions. Then, F_0 is determined in terms of the Lagrangian variables R_0, t from (3.14) in the form

$$\frac{\partial F_0}{\partial t} = -\left(\frac{Q}{Qt + R_0} + \frac{Q'}{Q't + 1} \right) F_0, \tag{3.17}$$

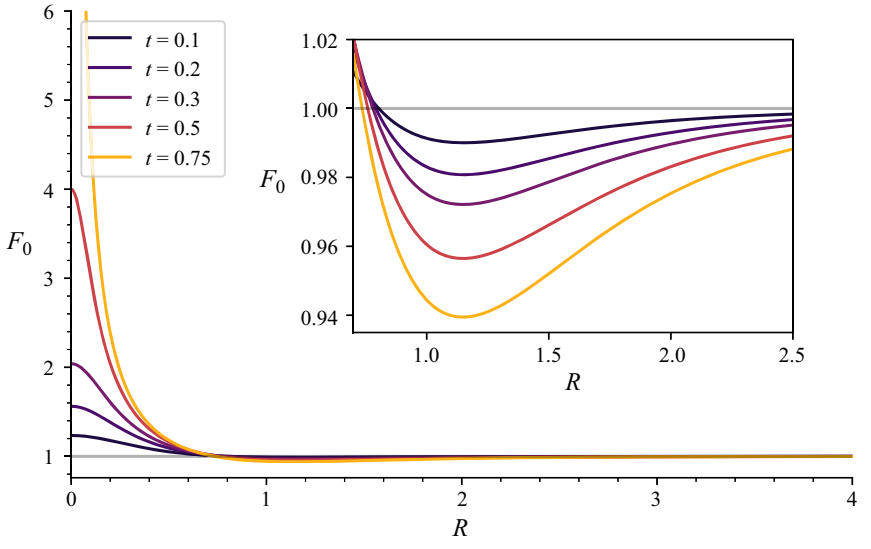

Figure 6. Value of F_0 plotted from (3.20) as a function of R for $t = 0, 0.1, 0.2, 0.3, 0.5, 0.75$.

where

$$Q = \frac{\partial \Phi_0}{\partial R} = -\frac{R_0}{(1 + {R_0}^2)^{5/2}}, \tag{3.18}$$

and

$$Q' = \frac{\mathrm{d}Q}{\mathrm{d}R_0}. \tag{3.19}$$

Hence, F_0 has a time dependence that is different from that in (2.26), namely

$$F_0 = \frac{R_0}{(R_0 + Qt)(1 + Q't)}, \tag{3.20}$$

so that F_0 grows like $(1 - t)^{-2}$ as $t \uparrow 1$ when $R = 0$. A typical profile for F_0 is shown in figure 6, which is geometrically similar to figure 2. However, when we calculate p as we did to derive (2.30), we find that

$$p = \left(\left(\frac{\partial^2 \Phi_0}{\partial R^2} \right)^2 + \frac{1}{R} \frac{\partial \Phi_0}{\partial R} \frac{\partial^2 \Phi_0}{\partial R^2} + \frac{1}{R^2} \left(\frac{\partial \Phi_0}{\partial R} \right)^2 \right) ({F_0}^2 - z^2). \tag{3.21}$$

The leading bracket is positive for all $R \geq 0$ and hence the only maximum of p is at $R = 0, z = 0$.

As for the two-dimensional case, if we let $R_0 \to 0$ and $t \to 1$, we find, from (3.15), (3.16) and (3.20) that, the scalings in (2.33*a–e*) need to be modified. For (3.1), (3.2), (3.3) the appropriate scalings are

$$1 - t = O(\epsilon^{2/7}), \quad r = O(\epsilon^{-4/7}), \quad z = O(\epsilon^{-4/7}), \quad f = O(\epsilon^{-4/7}) \quad \text{and} \quad \phi = O(\epsilon^{-10/7}). \tag{3.22a–e}$$

This means that ϕ still satisfies Laplace's equation and when we apply the matching condition analogous to (2.34*a*,*b*), the resulting lowest-order solution in this region emerges

as the limit of (3.6) as $t \uparrow 1$, namely

$$\phi = \frac{z^2 - \frac{1}{2}r^2}{1-t} - \frac{3}{5(1-t)^5} \quad \text{and} \quad f = \frac{1}{(1-t)^2}. \tag{3.23a,b}$$

Finally, we note that a small-time analysis when $d = O(1)$ again leads to a profile similar to that in figure 5 and that if we set $d = 1 + \delta$ where δ is small, then, for small times the jet length is of $O(t/\delta^3)$ as $\delta \to 0$, which is an order of magnitude longer than that in the two-dimensional case. This is to be expected since there is now flow into the jet from all directions.

4. Conclusion

This paper presents asymptotic evidence to suggest that, when a pressure maximum is close to a planar free boundary of an inviscid fluid in the absence of gravity, the surface can develop a fast jet. When the jets are driven by dipoles, they accelerate to become of infinite length in a finite time which becomes shorter as the initial distance between the dipoles decreases. The theory is described in both two dimensions and three dimensions and it is shown that axisymmetric jets accelerate faster than those in two dimensions.

These predictions are based on asymptotic analyses that only apply for certain stages of the jet evolution and numerical solutions are needed to corroborate our predictions and complete the picture.

Acknowledgements. The authors are grateful to Professor G. Sander for numerous helpful conversations and to M. Cotton who provided the figures.

Funding. This research received no specific grant from any funding agency, commercial or not-for-profit sectors.

Declaration of interests. The authors report no conflict of interest.

Author ORCIDs.
J.R. Ockendon https://orcid.org/0000-0002-8125-9350;
H. Ockendon https://orcid.org/0000-0001-8063-4537.

References

Cooker, M.J. 2002 Unsteady pressure fields which precede the launch of free-surface liquid jets. *Proc. Roy. Soc. Lond.* A **458**, 473–488.

Iafrati, A. & Korobkin, A.A. 2008 Hydrodynamic loads during early stage of flat plate impact onto water surface. *Phys. Fluids* **20**, 082104.

King, A.C. & Needham, D.J. 1994 The initial development of a jet caused by a fluid, body and free-surface interaction. Part 1. A uniformly accelerating plate. *J. Fluid Mech.* **268**, 89–101.

Longuet-Higgins, M.S. 1972 A class of exact, time-dependent, free-surface flows. *J. Fluid Mech.* **55**, 529–543.

Longuet-Higgins, M.S. 1975 Integral properties of periodic gravity waves of finite amplitude. *Proc. R. Soc. Lond.* A **342**, 157–174.

Needham, D.J., Billingham, J. & King, A.C. 2007 The initial development of a jet caused by a fluid, body and free-surface interaction. Part 2. An impulsively moved plate. *J. Fluid Mech.* **578**, 67–84.

Scolan, Y.-M. 2023 Some aspects of the pressure field preceding the onset of critical jets in a breaking wave. *J. Engng Maths* **138** (1).

Scolan, Y.-M. & Etienne, S. 2021 Properties of the pressure field in highly nonlinear free surface flows with critical jet. *J. Engng Maths* **128** (4).